Supplementary Information

Regulation of Anderson localization for enhancing thermoelectric properties in Mn doped $AgSbSe_2$ compounds

Yaqiong Zhong,[a] Keke Liu,[a] Shuo Chen,[a] Hao Sang,[a] Xili Wen,[a] Qingjie Zhang,[a] Jinsong Wu,[b] Pierre Ferdinand Poudeu Poudeu,[d] Xianli Su,[*a] Ctirad Uher,[c] Xinfeng Tang[*a]

[a]State Key Laboratory of Advanced Technology for Materials Synthesis and Processing, Wuhan University of Technology, Wuhan 430070, China.

[b]Nanostructure Research Center, Wuhan University of Technology, Wuhan 430070, China.

[c]Department of Physics, University of Michigan, Ann Arbor, Michigan 48109, United States.

[d]Laboratory for Emerging Energy and Electronic Materials (LE3M), Department of Materials Science and Engineering, University of Michigan, Ann Arbor, Michigan 48109, United States.

**Corresponding authors*: suxianli@whut.edu.cn; tangxf@whut.edu.cn

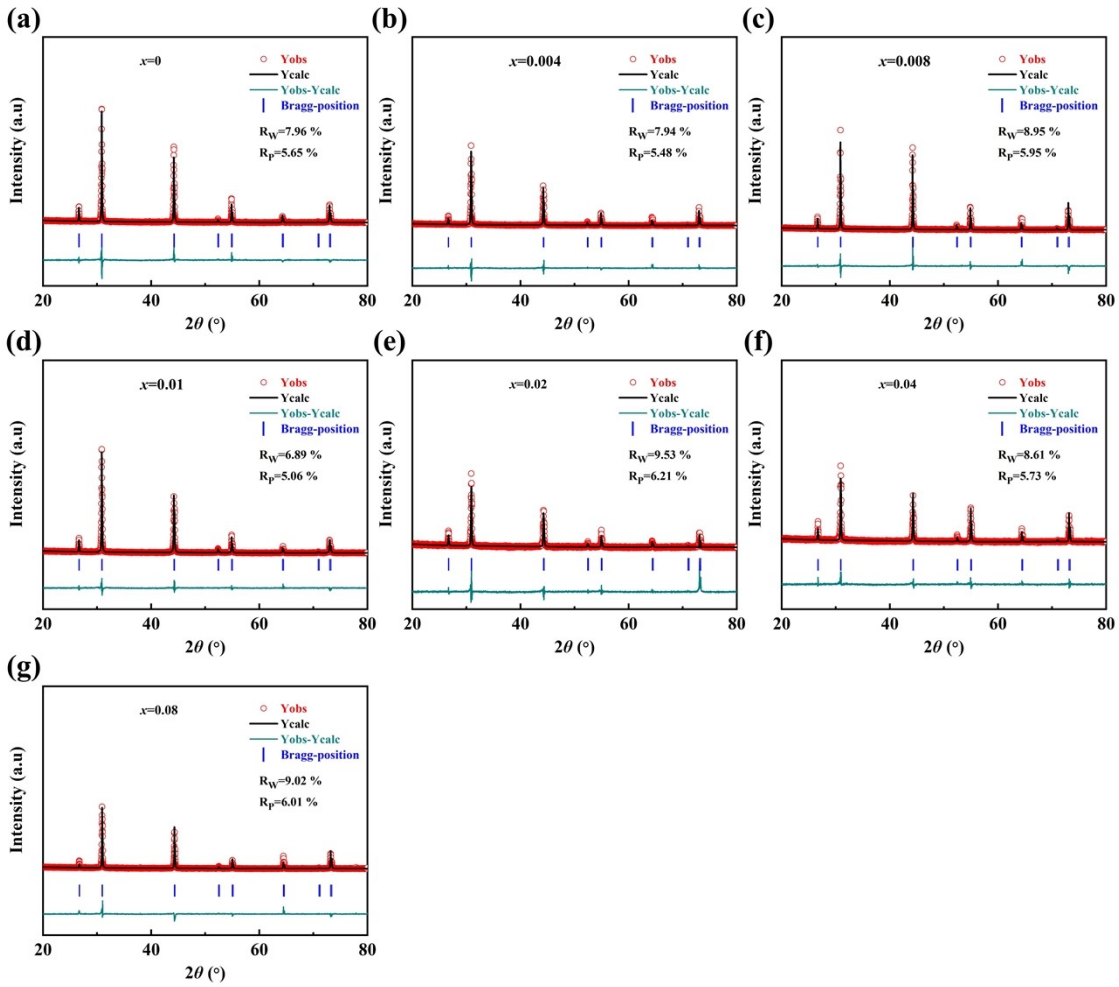

Fig. S1. Rietveld refinements of $AgSb_{1-x}Mn_xSe_2$.

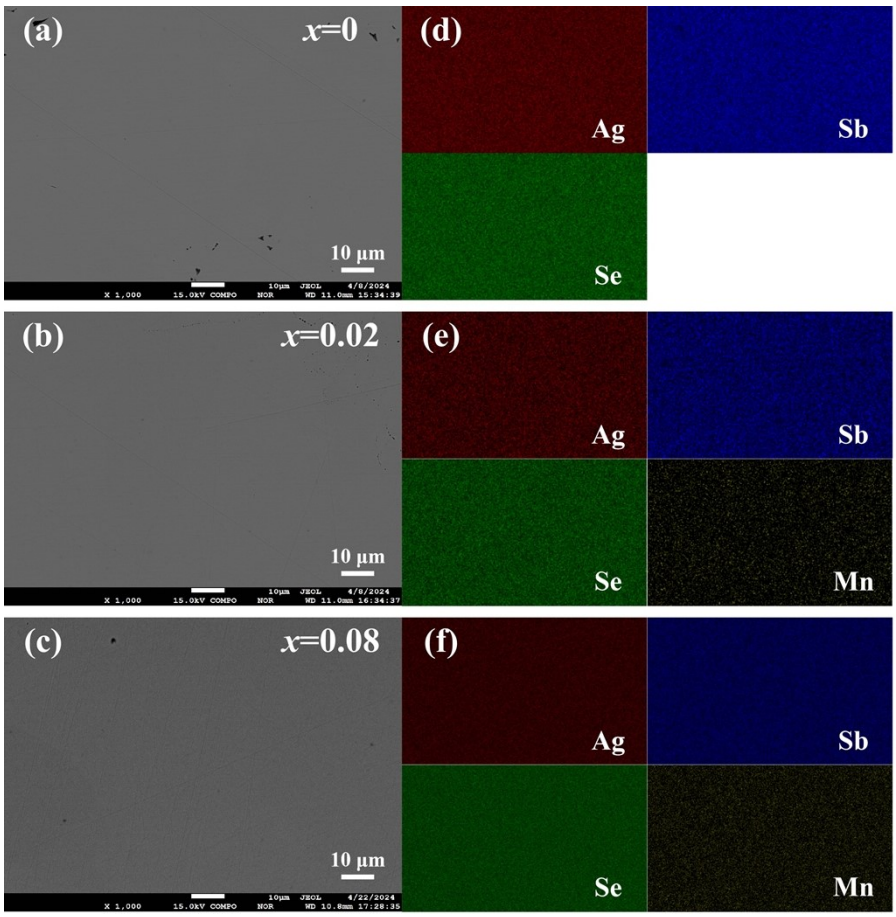

Fig. S2. (a)-(c) Back-scattered electron images and (d)-(f) energy-dispersive X-ray spectrometry elemental mappings of $AgSb_{1-x}Mn_xSe_2$.

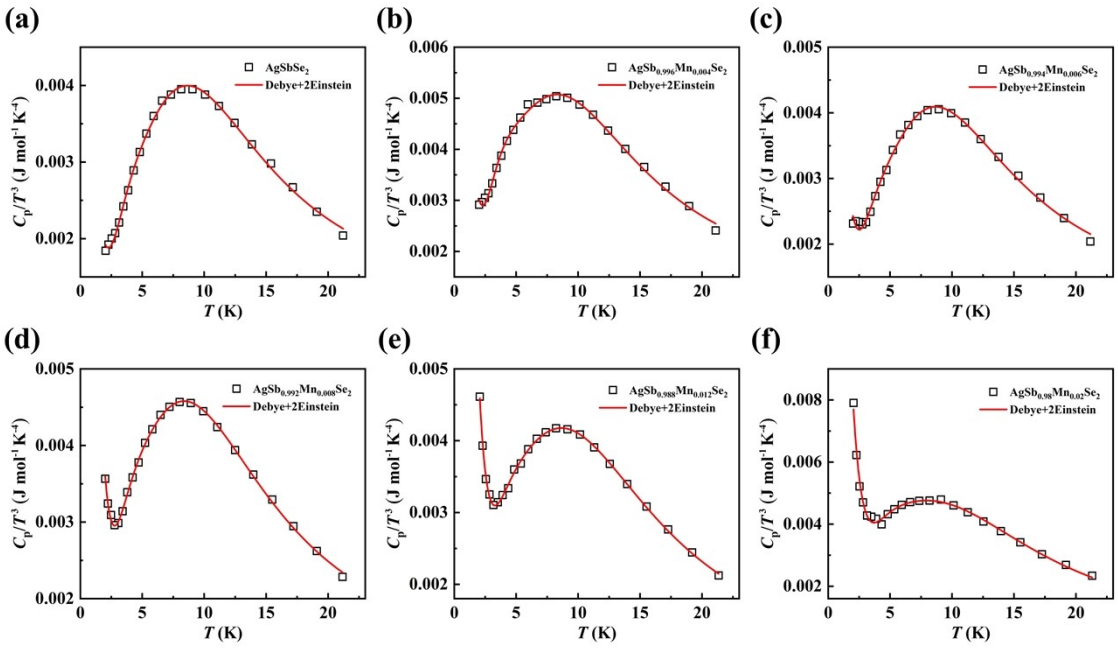

Fig. S3. The relationship between C_p/T^3 and T for $AgSb_{1-x}Mn_xSe_2$. The Boson peak can be fitted only with the combined Debye-2Einstein model.

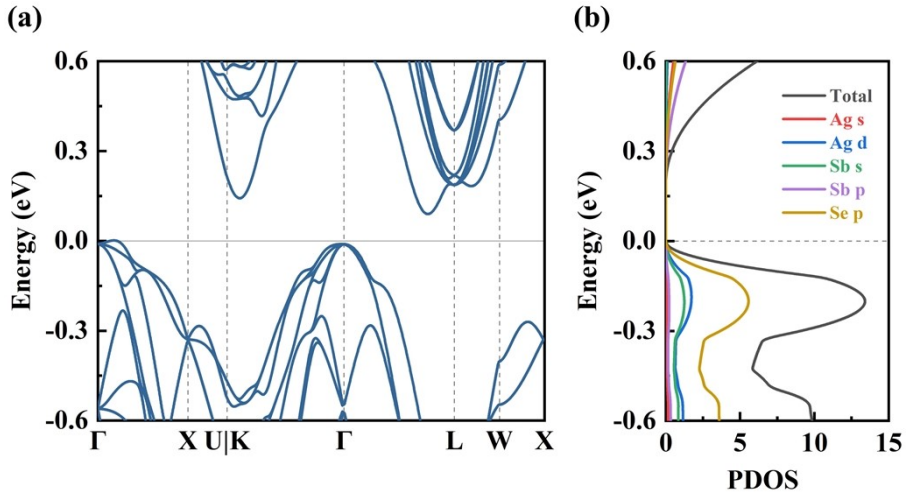

Fig. S4. Calculated band structure and PDOS of $Ag_{16}Sb_{16}Se_{32}$.

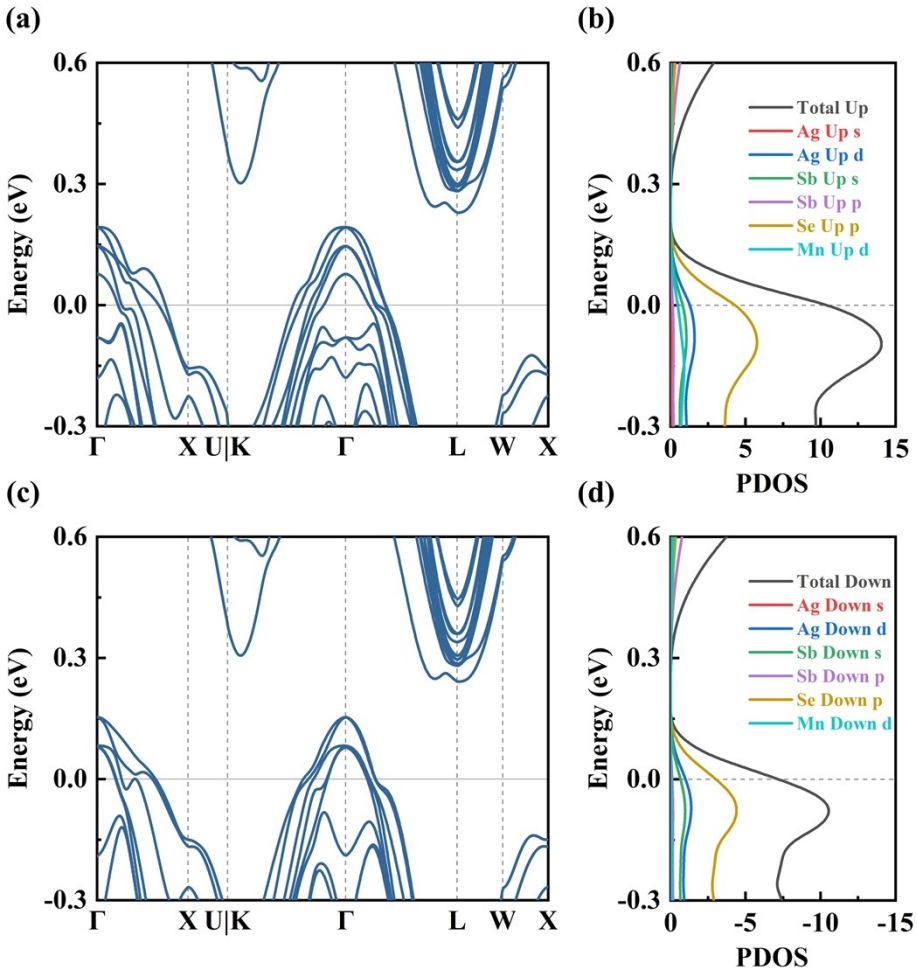

Fig. S5. Calculated band structure and PDOS of $Ag_{16}Sb_{15}MnSe_{32}$. (a)-(b) Spin-up, and (c)-(d) Spin-down.

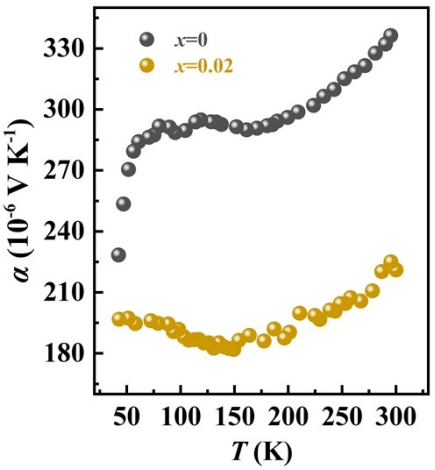

Fig. S6. Low temperature-dependent Seebeck coefficients (α) of pristine $AgSbSe_2$ and 2% Mn doped $AgSbSe_2$.

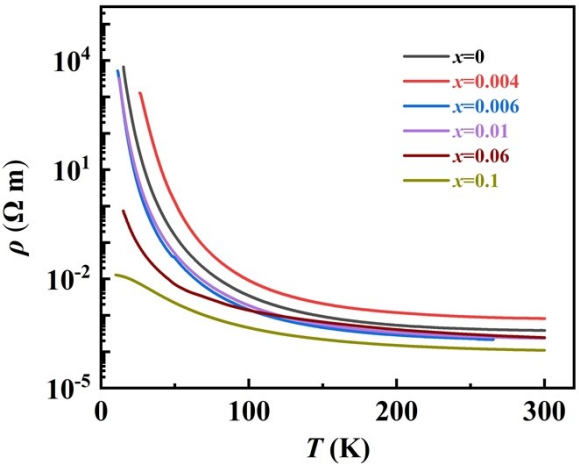

Fig. S7. Resistivity (ρ) *versus* T plots of the samples $AgSb_{1-x}Mn_xSe_2$.

Table S1. Low temperature heat capacity parameters of $AgSb_{1-x}Mn_xSe_2$. Here, γ is the Sommerfeld constant, b is the Debye lattice term, A_i and θ_{Ei} are the amplitude and the Einstein temperature of the ith Einstein oscillator mode.

Parameters	x=0	x=0.004	x=0.006	x=0.008	x=0.012	x=0.02
γ (mJ mol^{-1} K^{-2})	2.65	6.18	4.79	9.38	15.46	29.67
b (mJ mol^{-1} K^{-4})	1.2	1.29	1.18	1.2	0.92	0.62
A_1	1.23	1.56	1.25	1.8	2.28	3.9
θ_{E1} (K)	25.69	23.8	25.85	26.63	29.01	30.96
A_2	12.22	16.5	12.8	14.79	16.82	23.59
θ_{E2} (K)	51.07	51.46	51.1	52.81	57.01	62.03

Table S2. Basic parameters of the $\kappa_F\lambda$ *versus* T for $AgSbSe_2$

T (K)	σ (Ω^{-1} m^{-1})	n_H (10^{18} cm^{-3})	μ_w(cm^2 v^{-1} s^{-1})	$\kappa_F\lambda$
40	0.02	0.625	0.02	0.000125
60	0.614	3.37	0.11	0.00218
100	10.346	6.10	1.06	0.03
150	44.26	12	2.3	0.1029
300	224	18	7.3	0.45

Table S3. Basic parameters of the $\kappa_F\lambda$ *versus* T for $AgSb_{0.99}Mn_{0.01}Se_2$

T (K)	σ (Ω^{-1} m^{-1})	n_H (10^{18} cm^{-3})	μ_w(cm^2 v^{-1} s^{-1})	$\kappa_F\lambda$
14	0.66	9.4	0.00443	0.0007728
20	6.5	2.4	0.2065	0.01199
47	7.24	0.3	1.4731	0.0267
70	25	0.58	2.6694	0.07389
97	91	1.35	4.2032	0.20323
120	131	2.02	4.0501	0.2556
154	172	2.43	4.4230	0.3159
300	3015	3.7	50.89	4.8

Table S4. Summary of the physical parameters of $AgSb_{1-x}Mn_xSe_2$

Parameters	x=0	x=0.004	x=0.006	x=0.008	x=0.012	x=0.02
σ_{300K} (S m^{-1})	250	3823	2044	4350	5916	8246
$N(E_F)_{Cp}$ (m^{-3} J^{-1})	1.28×10^{45}	2.99×10^{45}	2.32×10^{45}	4.54×10^{45}	7.5×10^{45}	1.44×10^{46}